Journal of
Materials Chemistry C

Accepted Manuscript

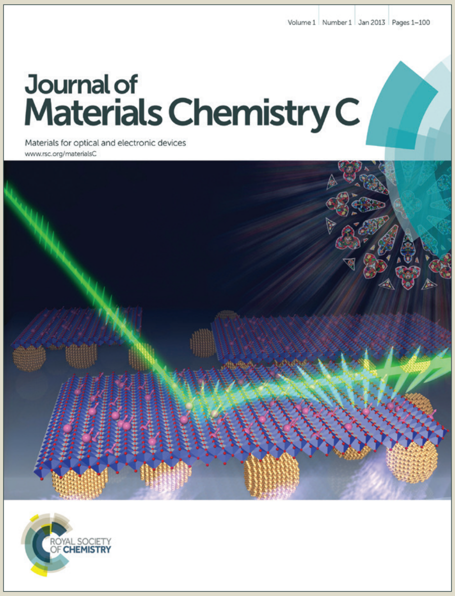

ROYAL SOCIETY
OF CHEMISTRY

www.rsc.org/materialsC

Journal of Materials Chemistry C RSCPublishing

PAPER

Cite this: DOI: 10.1039/x0xx00000x

Received 00th January 2012,
Accepted 00th January 2012

DOI: 10.1039/x0xx00000x

www.rsc.org/

Aluminium Nanoparticles Synthesized by a Novel Wet Chemical Method and Used to Enhance the Performance of Polymer Solar Cells by Plasmonics Effect

Yue Cui,[abc] Di Huang, †[ab] Yang Li, [ab] Wenxiao Huang,[c] Zhiqin Liang, [ab] Zheng Xu, [ab] and Suling Zhao [*ab]

To enhance the light harvesting of polymer solar cells (PSCs), amphipathic Al core and a PPh_3 protective shell ($Al@PPh_3$) nanoparticles (NPs) synthesized by a simple and facile wet chemical process are incorporated to the anode buffer layer of the PTB7:$PC_{71}BM$ blend PSCs. The optimized power conversion efficiency (PCE) of 6.29% is achieved, which is enhanced about 20% comparing with the pristine device. It is attributed to the localised surface plasmon resonance (LSPR) effects of $Al@PPh_3$ NPs incorporated in the buffer layer and the light absorption of devices are enhanced.

1. Introduction

Polymer solar cells (PSCs) have many advantages over their inorganic counterparts, including low fabrication costs and application versatility[1-3]. However, the PCE at present is significantly low, which is mostly limited by poor carrier mobility of organic materials[4]. A thinner PSCs active layer can lower the probability of charge recombination and increase the carrier drift velocity, while a minimum film thickness is always required to ensure sufficient photon absorption. Therefore, it's quite important to increase the absorption of active layer without increasing the thickness.

An effective method for achieving light trapping inside PSCs to increase the absorbance is the use of metallic NPs that produce localised surface plasmon resonance (LSPR), which is excitated through the resonant interaction between the local electromagnetic fields of incident light and the surface electron density surrounding metallic NPs causes local enhancement in the electromagnetic field. It has been well-established that noble metal (Au and Ag) NPs act a significant impact on the enhancement in the power conversion efficiency (PCE) of PSCs with different structures by the LSPR effects[5-10].

Comparing with the noble metals, Al, which is also capable of supporting LSPR and significantly more abundant and cheaper, has attracted a surging interest in fundamental studies and applications. Recent studies[11] suggested that Al NPs have the potential to yield significantly greater enhancement than the typical plasmonics materials, due to the much higher plasma frequency, which ensures a better overlap between plasmon resonance and absorption band of organic semiconductors. Al NPs also can enhance stability of PSCs[12]. Despite all these potential advantages, the exploitation of Al NPs for LSPR is in a fledging period and still facing many challenges. LSPR is sensitive to the size, shape, interparticle spacing, dielectric environment and dielectric properties of used nanoparticles. However it's challenging to prepare Al NPs with air stability, narrow size distribution and low degree of aggregation. Simultaneously, Al NPs are vulnerable when exposure to ambient conditions: an oxidized layer on the particles' surface is formed as a barrier suppressing further oxidation, which decreases the effect of LSPR on the performance of of PSCs due to undesirable exciton quenching processes[13].

Although both positive and negative effects[14] of introducing metallic NPs into PSCs have been reported, the incorporation of cheaper metallic NPs into the photoactive layer or the interconnecting layer is still an potential method to improve the performance of PSCs with different structures. So in this paper, a novel architecture of Al core and a PPh_3 protective shell (Al@PPh_3) nanoparticles (NPs) have been synthesized by a simple and facile wet chemical processfor realizing LSPR to enhance PSCs efficiencies. The influence of various Al@PPh_3 NPs shape and configurations were investigated. In particular, poly[[4,8-bis[(2-ethylhexyl)oxy]benzo[1,2-b:4,5-b']dithiophene-2,6-diyl][3-fluoro-2-[(2-ethylhexyl)carbonyl]thieno[3,4-b]thiophenediyl]] (PTB7) was chosen as the electron donor material and the prepared Al@PPh_3 NPs were incorporated in anode buffer layer for the first time.

2. Experimental Section

2.1 Synthesis and characteristic of Al@PPh_3 NPs

Aluminium chloride ($AlCl_3$, anhydrous, powder, 99.99%, trace metals basis), lithium aluminium hydride ($LiAlH_4$, powder, reagent grade), triphenylphosphine (PPh_3, powder, ReagentPlus grade) were purchased from Sigma-Aldrich Chemical and used as received without any purification. $AlCl_3$ and $LiAlH_4$ were acted as the precursor for preparing the Al particles, while PPh_3 was acted as both stabilizing ligand and reduction agent. 1,3,5-trimethylbenzene solution (analytical standard) which was dealing with the ultrasonic cleaning and dehydration process was used as the solvent for the reaction of the chemicals.

In glovebox, $AlCl_3$ (2 mmol) and PPh_3 (40 mmol) were mixed with 50 mL of 1,3,5-trimethylbenzene in a bottom flask, and stirred for 0.5 h. Then 10 ml of 1,3,5-trimethylbenzene containing $LiAlH_4$ (6mmol) was slowly added to the flask. . Subsequently, the precursor solution was removed from glovebox and heated to 164 ℃ and maintained for 1 h. All reactions were under argon protection. The prepared Al@PPh_3 NPs were extracted by a centrifugation process at 12000 r.p.m for 10 min, and washed with 0 ℃ methyl alcohol and tetrahydrofuran (THF) several times.

In order to identify the crystallization phase, X-ray diffraction (XRD) analysis was carried out by a D8 FOCUS X-raly diffractometer with Cu Kα irradiation (λ=1.5406 Å). The scanning angle range (2θ) started from 20° to 90° at a speed of 0.05°/s. The surface structures of the Al@PPh_3 NPs were observed by a scanning electron microscopy (SEM, Hitachi, S-4300). The transmission electron microscopy (TEM) and high-resolution transmission electron microscopy (HRTEM) images were recorded by a JEM-2100F microscopy operated at 200 kV. The Fourier transform infrared (FT-IR, Thermo Fisher Scientific, Nicolet-6700) spectroscopy with the KBr pellet was performed to investigate whether the PPh_3 layer was well covered on the surface of Al@PPh_3 NPs.

2.2 Fabrication of PSCs

The indium tin oxide (ITO) glass substrates (sheet resistance 15 Ω/□) were cleaned consecutively in ultrasonic baths containing acetone, ethanol and de-ionized water and dried by high pure nitrogen gas. The pre-cleaned ITO substrates were then treated with UV-ozone for 5 min. Electron donor material PTB7 and electron acceptor $PC_{71}BM$ were purchased from 1-material Chemscitech and Nano-C, respectively, and used as received. The Al@PPh_3 NPs were dissolved in ethyl alcohol with a concentration of 0.1mmol ml^{-1}. The poly-(3,4-ethylenedioxythiophene)-poly-(styrenesulfonate) (PEDOT:PSS) purchased from H.C. Starck co. Ltd. The device structures were ITO/Al@PPh_3 NPs/PEDOT:PSS/PTB7:$PC_{71}BM$(1:1.5 by weight)/LiF/Al, ITO/Al@PPh_3 NPs：PEDOT:PSS/PTB7:$PC_{71}BM$/LiF/Al and the regular device structure was ITO/PEDOT:PSS/PTB7:$PC_{71}BM$/LiF/Al.All anode buffer layers were spin-coated on the ITO substrates under 3000 rpm for 40 s. Then those ITO substrates were dried in air at 120 ℃ for 10 min and then transferred to an N_2 glove box and dried again at 120 ℃ for 10 min on a hot plate. The polymer materials PTB7 and $PC_{71}BM$ were dissolved in chlorobenzene with a concentration of 20 mg ml^{-1}, respectively. The PTB7:$PC_{71}BM$ active blend layer was prepared by spin-coating a mixed solvent of chlorobenzene/1,8-diiodoctane (97:3 by volume) solution (concentration, 20 mg ml^{-1}) at 1,000 r.p.m. for 2 min. The 0.7 nm interfacial layer LiF and aluminium cathode layer of about 100 nm were successively deposited by thermal evaporation under $2*10^{-4}$ Pa vacuum conditions.. The active area is about 9 mm^2, which is defined by the vertical overlap of ITO anode and Al cathode.

The current–voltage characteristics of PSCs were measured using a Keithley 4200 semiconductor characterization system and ABET Sun 2000 solar simulator. The external quantum efficiency (EQE) spectra were measured on Zolix Solar Cell Scan 100. The absorption spectra of films were measured with a Shimadzu UV-3101 PC spectrometer. The thicknesses of PTB7: $PC_{71}BM$ was about 80 nm which was determined by the KLA Tencor P6 stylus profiler.

3. Results and discussion

Amphipathic Al@PPh_3 NPs were synthesized by a novel wet chemical process, and the morphological control with surfactant PPh_3 have been discussed. The reaction was explained as the following equation (1):

$$LiAlH_4 + AlCl_3 \xrightarrow{PPh_3} Al@PPh_3 + LiCl + H_2 \quad (1)$$

X-ray diffraction (XRD) analysis (Fig. 1a) confirmed the face-centered-cubic (fcc) Al@PPh_3 NPs, which agreed with the JCPDS (NO.:04-0787) , and showed no appearance of Al_2O_3.

The morphology investigation is demonstrated in Fig. 1b. The HRTEM image revealed the core-shell structure with an Al core and a 5 nm thick amorphous PPh_3 protective shell, which was also confirmed by the Fourier transform infrared spectrometry (FT-IR) spectra (see ESI, Fig. S1).

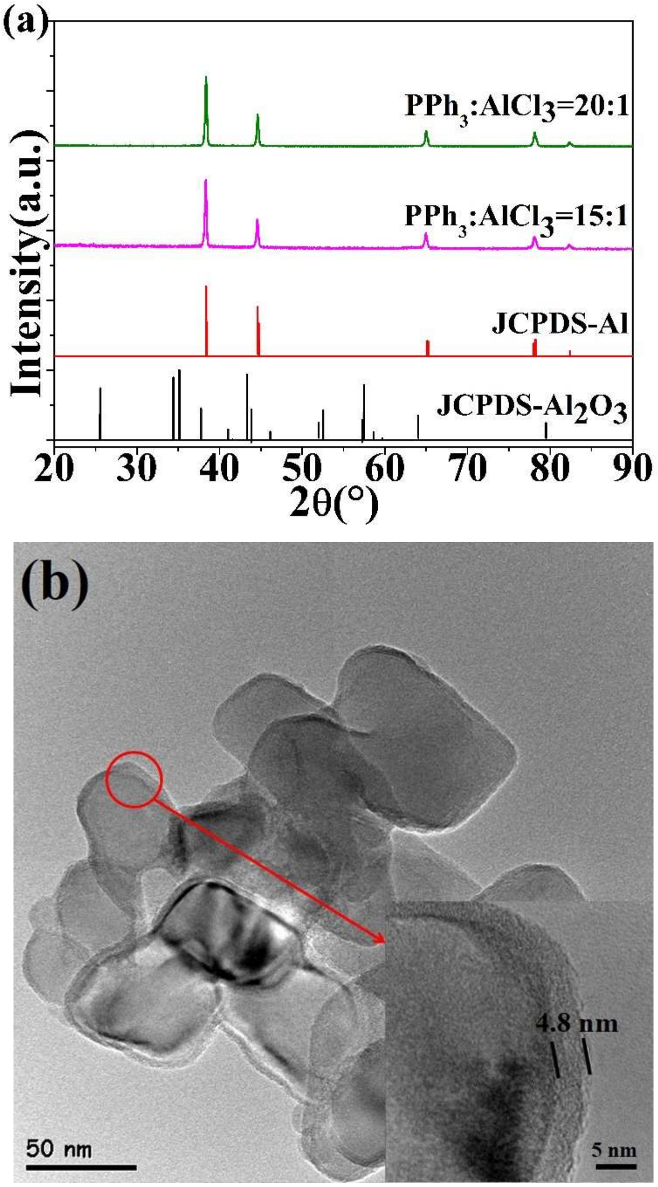

Fig.1. (a) XRD patterns of prepared Al@PPh$_3$ NPs (b) TEM and HRTEM images of Al@PPh$_3$ NPs with PPh$_3$:AlCl$_3$=20:1

PPh$_3$ played multiple roles: firstly, it's expected to prevent the aggregation of nanoparticles and leads to a small particle size (see ESI, Fig. S2 and S3). Secondly, PPh$_3$ provided the solubility of Al@PPh$_3$ NPs in both aqueous and oleic phase, which is a key to fabricate the PSCs with different structure.

Then the prepared Al@PPh$_3$ NPs were introduced into PTB7:PC$_{71}$BM based PSCs to act as the anode buffer layer. The volume ratio of the Al@PPh$_3$ NPs aqueous solution and the PEDOT:PSS aqueous solution is 1:3. **Fig. 2a** and **Fig. S4** show the photovoltaic device structure and the molecular structure of used materials PTB7 and PC$_{71}$BM, respectively. **Fig. 2b** displays the photocurrent-voltage (J-V) characteristics, recorded under 100 mW cm^{-2} illumination (AM 1.5G), of the PSCs prepared with different anode buffer layers. The respective averaged photovoltaic characteristics are summarized in **Table 1**.

Interestingly, it's observed that the incorporation of Al@PPh$_3$ NPs into the buffer layer induces an enhancement of nearly 5.9% to the short-circuit current (Jsc), and a noticeably upward trend in the values of fill factor (FF), while the open-circuit voltage (Voc) remains a constant almostly. The devices with Al@PPh$_3$ NPs exhibits a PCE of 6.29%, which is nearly 19.6% higher than the pristine device.

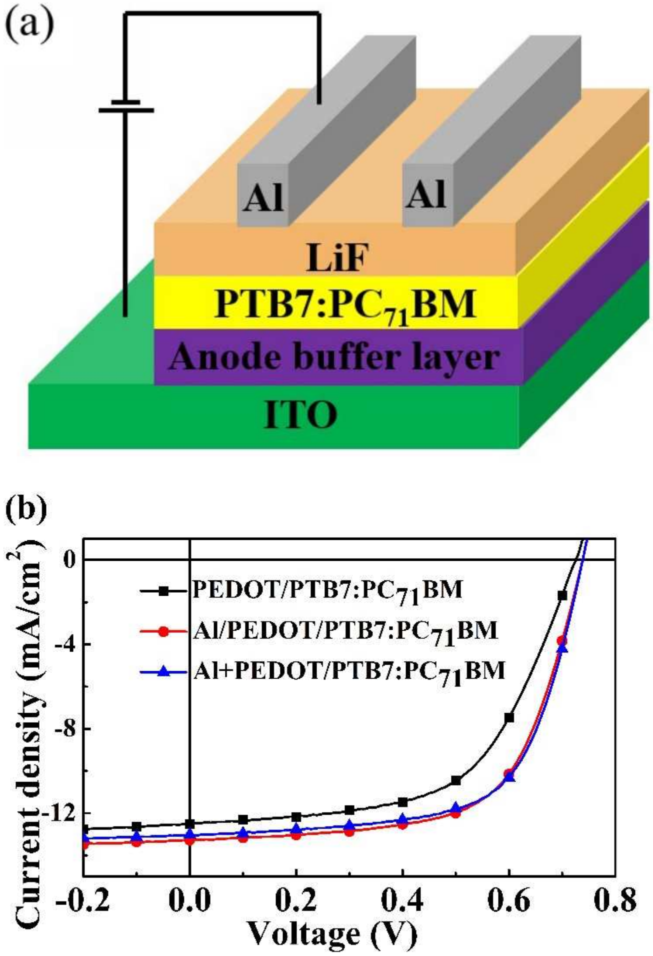

Fig. 2. (a) schematic structure of PTB7:PC71BM blend PSCs. (b) *J–V* characteristic curves of PSCs with different buffer layers under illumination of AM 1.5 G, 100 mW cm^{-2}

Table 1. Key photovoltaic parameters of PSCs with different anode buffer layers

Anode buffer layers	V_{oc} [V]	J_{sc} [mA/cm^2]	FF [%]	PCE [%]	Rsh (ohm. cm^{-2})	Rs (ohm. cm^{-2})
Pristine PEDOT:PSS	0.73±0.01	12.53±0.16	57.5±0.01	5.26±0.03	665.37	13.94
Al@PPh$_3$ NPs / PEDOT:PSS	0.74±0.01	13.27±0.15	63.9±0.12	6.28±0.02	943.61	10.49
Al@PPh$_3$ NPs + PEDOT:PSS	0.74±0.01	13.02±0.09	65.3±0.05	6.29±0.02	1063.01	8.31

In order to find a optimal concentration, we also studied the volume ratio of 0:1, 1:2, 1:3, 1:4 and 1:9 of the Al@PPh$_3$ NPs aqueous solution and the PEDOT:PSS aqueous solution according to the photovoltaic performance. The data is shown in Fig. S5 and Table S1. We found that the optimized volume ratio is 1:3. Further increasing of Al@PPhs$_3$ NPs leads to a detrimental effect on the PCE.

In order to get an insight for the mechanism to the enhanced performance of the short-curcuit current, the incident photon-to-electron conversion efficiency (IPCE) curve and absorption spectra of the Al@PPh$_3$ NPs were measured and compared with that of the pristine one (Fig.3). The improvement in the IPCE, which is broad and uniform ranging from 350 to 700 nm, results from the effect of Al@PPh$_3$ NPs, especially from the efficient light scattering and improved charge transport. The photocurrent increased notably after incorporating the Al@PPh$_3$ NPs, which implies that more light was harvested because of multiple light scattering by the Al@PPh$_3$ NPs.[15] To confirm this hypothesis we measured optical absorption spectra of Al@PPh$_3$ NPs, as well as the devices fabricated with and without Al@PPh$_3$ NPs in PEDOT:PSS (showed in Fig. 3b). In addition, the increased and extended operability of Al@PPh$_3$ NPs-PEDOT:PSS composite PSCs at visible wavelengths well below the UV region is closely related to the injection of plasmonically excited hot carriers (electrons) from metal NPs into PEDOT:PSS.[16] The wavelength range of spectral response enhancement coincides with the improvement in the IPCE, indicating that excitation of the LSPR indeed improved the photocurrent.

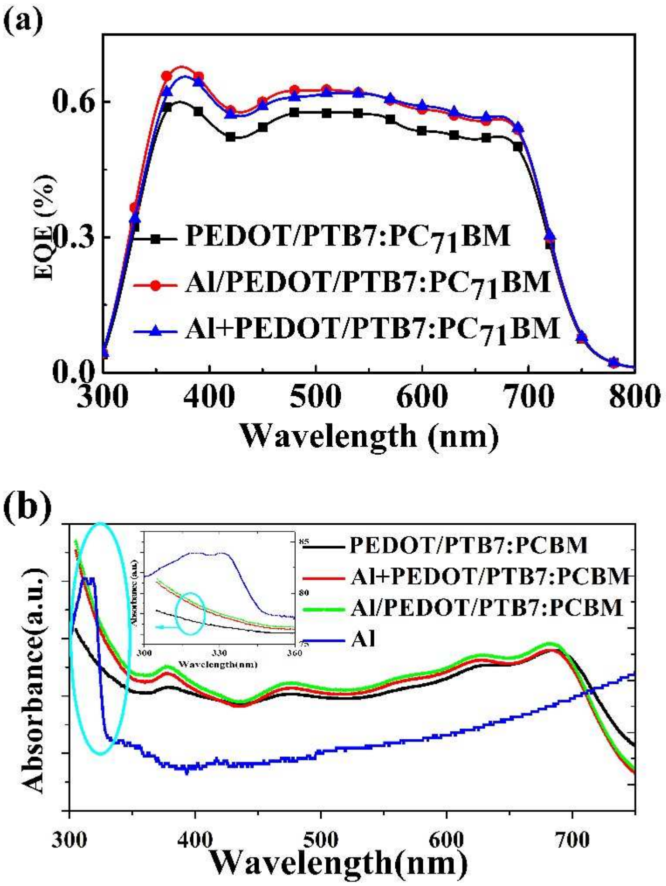

Fig. 3. (a) IPCE of devices, respectively; (b) Absorption spectra of Al@PPh$_3$ NPs and Al@PPh$_3$ NPs with and without embedding in PEDOT:PSS

To further investigate the underlying mechanism responsible for the enhanced performance of the devices, we compared the maximum exciton generation rates (Gmax) and exciton dissociation probabilities for devices prepared using pristine PEDOT:PSS solution and the devices with Al@PPh$_3$ NPs/PEDOT:PSS two anode buffer layers, following the analytical approach reported by Mihailetchi and Chen.[17-19] Fig. 4 should reveal the effect of the LSPR on the photocurrent density (Jph) . the value of Jph using the equation Jph =JL-JD, where JL and JD are the current densities under illumination and in the dark, respectively. The plot of Jph with respect to the effective voltage Veff=Vo-V, where Vo is the compensation voltage at which Jph equals zero and V is the applied voltage. Jph reaches saturation for both devices, suggesting all photogenerated excitons are dissociated into free carriers and all carriers are collected at the electrodes without any bimolecular recombination.[20-22] The saturation photocurrent density (Jsat) correlates with the value of Gmax, given by Jsat =qGmaxL, where q is the electronic charge and L is the thickness of the active layer. From Fig. 4, we know the value of Jsat for the device with Al@PPh$_3$ NPs/PEDOT:PSS two layers was higher than the device prepared with pristine PEDOT:PSS solution,then the calculated values of Gmax have the same trend. Because the value of Gmax is governed only by the absorption of light,[17-19] the enhanced value suggests that the incorporation of the Al@PPh$_3$ NPs increased the degree of light harvesting in the devices. From Fig. 4, the saturation photocurrent density (J_{sat}) is 13.2 mA/cm^2 for the device prepared with pristine PEDOT:PSS solution while 13.8 mA/cm^2 for the device with Al@PPh$_3$ NPs/PEDOT:PSS doublelayers, respectively. The increased J_{sat} should be attributed to the effective charge carrier transport and collection of the PSCs with Al@PPh$_3$ NPs/PEDOT:PSS double layers.[23] Moreover, J_{sat} correlates with the value of G_{max}, given by $J_{sat} = qG_{max}L$, where q is the electronic charge and L is the thickness of the active layer.Then the calculated values of G_{max} for the devices were 9.93×10^{27} m^{-3}s^{-1}and 1.04×10^{28}m^{-3}s^{-1}, respectively. G_{max} slightly increased, suggesting that the incorporation of the Al@PPh$_3$ NPs increased the degree of light harvesting in the devices.;[24] Because the value of G_{max} is governed only by the absorption of light,[17-19] this well matched the enhanced absorption

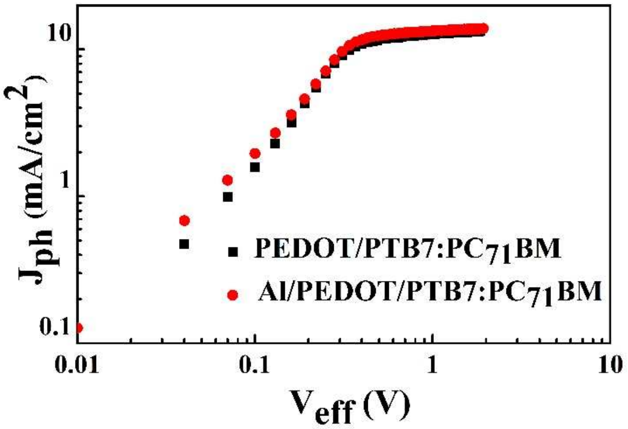

Fig. 4. Photocurrent density versus effective voltage (J_{ph}-V_{eff}) characteristics of devices prepared using pristine PEDOT:PSS solution and the devices with Al@PPh$_3$ NPs/PEDOT:PSS two anode buffer layers

Since the ratio J_{ph}/J_{sat} is essentially the product of exciton dissociation efficiency and charge collection efficiency,[18, 25] Under the shortcircuit condition (V = 0 V), Jph/Jsat almost is 90% for the devices with Al@PPh$_3$ NPs/PEDOT:PSS two anode buffer layers while it is only 87% for device prepared using pristine PEDOT:PSS solution（J_{ph} at V_{eff} = 0.5V）, indicating that excitation of the LSPR facilitated the excitons to dissociate into free carriers.[8] Generally speaking, a decreased Jph/Jsat suggests either a reduced exciton dissociation efficiency or charge collection efficiency, with the latter suggesting that bimolecular recombination begins to dominate and usually lead to a lower FF of PSCs.[21, 22] What more, from **Table 1**, we know Rsh of the Al@PPh$_3$ NPs devices are higher than the undoped device, which also means the increasing exciton dissociation efficiency after adding Al@PPh$_3$ NPs into the devices,[8] then lead to a higher FF of PSCs. Meanwhile the smaller Rs signifies a lower semiconductor bulk resistance, a better metal/semiconductor interfaces was induced by adding Al@PPh$_3$ NPs. Moreover, the reduced contact resistance can facilitate the electron extraction in PSCs.[26]

Conclusions

To summarize, for the first time we synthesized an amphipathic Al@PPh$_3$ NPs with core-shell structure to improve light harvesting in PSCs with a simple and facile wet chemical process. We have improved the device PCE 20% (from 5.26% to 6.29%), as well as the Jsc, FF and .These improvements result from a combination of enhanced light absorption caused by the LSPR of Al@PPh$_3$ NPs. From the observed increase in the FF, we deduced that excitation of the LSPR increased not only the rate of exciton generation but also the probability of exciton dissociation. Also, it is worthy to mention that those improvements exist even when Al@PPh3 NPs exhibit slight aggregation which is believed detrimental to the enhancement of the performance of PSCs. An even better outcome could be expected when the aggregation issue is restrained. Therefore, we have demonstrated that Al, as a cheap metallic material, is an excellent candidate to benefit the development of polymer solar cell.

Acknowledgements

We express the thanks to the Research Fund for the Doctoral Program of Higher Education No. 20120009130005 and the Fundamental Research Funds for the Central Universities with the Grant No. 2012JBZ001.

Notes and references

[a] Key Laboratory of Luminescence and Optical Information, Beijing Jiaotong University, Ministry of Education, Beijing 100044, PR. China.
[b] Institude of Optoelectronic Technology, Beijing Jiaotong University, Beijing 100044, PR. China.
[c] Center for Nanotechnology and Molecular Materials, Department of Physics, Wake Forest University, Winston-Salem, NC, USA
* Corresponding authors
Email addresses: slzhao@bjtu.edu.cn
† The first two authors contributed equally to this work

Electronic Supplementary Information (ESI) available: [details of any supplementary information available should be included here]. See DOI: 10.1039/b000000x/

1. Z. He, C. Zhong, S. Su, M. Xu, H. Wu and Y. Cao, *Nat. Photonics*, 2012, **6**, 591-595.
2. S. Obuchovsky, I. Deckman, M. Moshonov, T. S. Peretz, G. Ankonina, T. J. Savenije and G. L. Frey, *Journal of Materials Chemistry C*, 2014, **2**, 8903-8910.
3. A. Abrusci, S. D. Stranks, P. Docampo, H.-L. Yip, A. K.-Y. Jen and H. J. Snaith, *Nano Lett.*, 2013, **13**, 3124-3128.
4. G. Kakavelakis, E. Stratakis and E. Kymakis, *Chem. Commun.*, 2014.
5. X. Li, W. C. Choy, L. Huo, F. Xie, W. E. Sha, B. Ding, X. Guo, Y. Li, J. Hou and J. You, *Adv. Mater.*, 2012, **24**, 3046-3052.
6. D. D. Fung, L. Qiao, W. C. Choy, C. Wang, E. Wei, F. Xie and S. He, *J. Mater. Chem.*, 2011, **21**, 16349-16356.

7. F. X. Xie, W. C. Choy, C. C. Wang, E. Wei and D. D. Fung, *Appl. Phys. Lett.*, 2011, **99**, 153304.
8. J.-L. Wu, F.-C. Chen, Y.-S. Hsiao, F.-C. Chien, P. Chen, C.-H. Kuo, M. H. Huang and C.-S. Hsu, *ACS Nano*, 2011, **5**, 959-967.
9. C. Charlie, C. Wallace, D. Dixon and E. Wei, *J. Mater. Chem.*, 2012, **22**, 1206-1211.
10. Y. Zhang, J. Hao, X. Li, S. Chen, L. Wang, X. Li and W. Huang, *Journal of Materials Chemistry C*, 2014, **2**, 9303-9310.
11. G. Maidecchi, G. Gonella, R. Proietti Zaccaria, R. Moroni, L. Anghinolfi, A. Giglia, S. Nannarone, L. Mattera, H.-L. Dai and M. Canepa, *ACS Nano*, 2013, **7**, 5834-5841.
12. G. Kakavelakis, E. Stratakis and E. Kymakis, *RSC Adv.*, 2013, **3**, 16288-16291.
13. G. H. Chan, J. Zhao, G. C. Schatz and R. P. V. Duyne, *The Journal of Physical Chemistry C*, 2008, **112**, 13958-13963.
14. K. Topp, H. Borchert, F. Johnen, A. Tunc, M. Knipper, E. Von Hauff, J. Parisi and K. Al-Shamery, *The Journal of Physical Chemistry A*, 2009, **114**, 3981-3989.
15. S.-W. Baek, J. Noh, C.-H. Lee, B. Kim, M.-K. Seo and J.-Y. Lee, *Scientific reports*, 2013, **3**.
16. D. Zhang, W. C. Choy, F. Xie, W. E. Sha, X. Li, B. Ding, K. Zhang, F. Huang and Y. Cao, *Advanced Functional Materials*, 2013, **23**, 4255-4261.
17. F.-C. Chen, J.-L. Wu, C.-L. Lee, Y. Hong, C.-H. Kuo and M. H. Huang, *Applied Physics Letters*, 2009, **95**, 013305.
18. V. Mihailetchi, L. Koster, J. Hummelen and P. Blom, *Physical review letters*, 2004, **93**, 216601.
19. V. D. Mihailetchi, H. Xie, B. de Boer, L. A. Koster and P. W. Blom, *Advanced Functional Materials*, 2006, **16**, 699-708.
20. J. Peet, J. Kim, N. E. Coates, W. L. Ma, D. Moses, A. J. Heeger and G. C. Bazan, *Nature materials*, 2007, **6**, 497-500.
21. C. Shuttle, R. Hamilton, B. O'Regan, J. a. Nelson and J. Durrant, *Proceedings of the National Academy of Sciences*, 2010, **107**, 16448-16452.
22. Z. He, C. Zhong, X. Huang, W. Y. Wong, H. Wu, L. Chen, S. Su and Y. Cao, *Advanced Materials*, 2011, **23**, 4636-4643.
23. F. Zhang, Z. Zhuo, J. Zhang, X. Wang, X. Xu, Z. Wang, Y. Xin, J. Wang, J. Wang and W. Tang, *Solar Energy Materials and Solar Cells*, 2012, **97**, 71-77.
24. L. Lu, T. Xu, W. Chen, J. M. Lee, Z. Luo, I. H. Jung, H. I. Park, S. O. Kim and L. Yu, *Nano letters*, 2013, **13**, 2365-2369.
25. V. Shrotriya, Y. Yao, G. Li and Y. Yang, *Applied physics letters*, 2006, **89**, 063505-063505-063503.
26. F.-x. Xie, W. C. Choy, E. Wei, D. Zhang, S. Zhang, X. Li, C.-w. Leung and J. Hou, *Energy & Environmental Science*, 2013, **6**, 3372-3379.

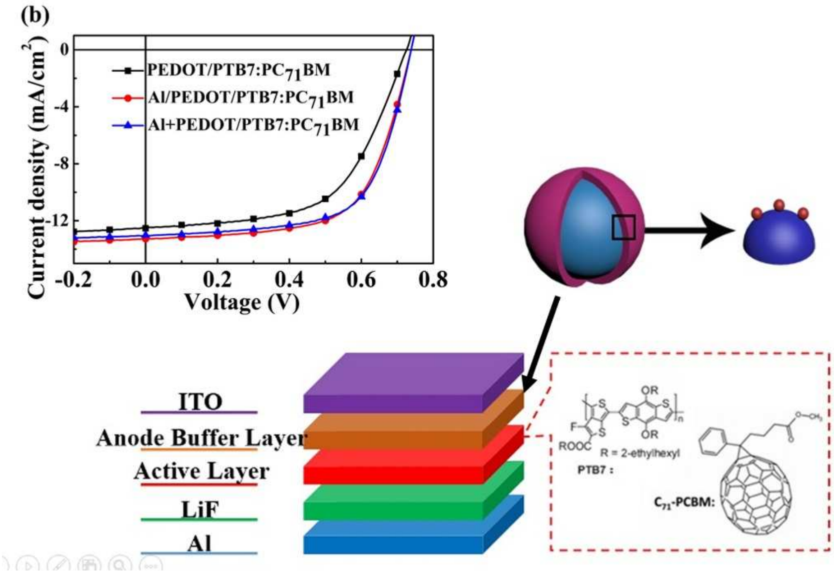

Amphipathic Al core and a PPh$_3$ protective shell nanoparticles synthesized by a simple and facile wet chemical process are incorporated to the anode buffer layer of the PTB7:PC$_{71}$BM blend PSCs with a enhancement about 20% of power conversion efficiency of polymer solar cells